

## Functionality, physicochemical properties, and applications of chitosan/nano-hydroxyapatite–tea polyphenol films

Dan Qiu<sup>a</sup>, Jingxuan Zhou<sup>a</sup>, Qiaohui Feng<sup>a</sup>, Kun Ren<sup>a</sup>, Hongying Zhang<sup>a</sup>, Yanfu He<sup>a,\*</sup>,  
Chuan Li<sup>a</sup>, Jing Liu<sup>b,\*</sup>, Nga Thi Tuyet Mai<sup>c</sup>

<sup>a</sup> College of Food Science and Engineering, Hainan University, 58th Renmin Road, Meilan District, Haikou 570100, Hainan Province, China

<sup>b</sup> School of Public Health, Hainan Medical University, Haikou 571199, Hainan, China

<sup>c</sup> Faculty of Food Technology, Nha Trang University, 02 Nguyen Dinh Chieu St., Nha Trang City, Viet Nam

### ARTICLE INFO

#### Keywords:

Chitosan-nano hydroxyapatite-tea polyphenol (CS-HAP-TP) films  
Physicochemical properties  
Sustained-release performance  
Antioxidant activity  
Preservation  
Flavor

### ABSTRACT

An active chitosan (CS) film containing a nano-hydroxyapatite–tea polyphenol (HAP-TP) complex was designed and prepared. The effects of HAP-TP loading on the structural and physicochemical properties of the CS-based film were evaluated. The mechanical and thermal properties of the film were significantly improved by the resulting intermolecular interactions and formation of hydrogen bonds between HAP-TP and CS, which reduced the water vapor and oxygen permeabilities of the film by 29.78 and 35.59 %, respectively. The CS-HAP-TP film exhibited excellent slow-release behavior and antioxidant activity, with a cumulative release rate at 700 h 6.79 % lower than that of CS-TP films. The CS-HAP-TP film significantly inhibited the deterioration of semi-dried golden pompano, and thus helped to retain the taste of umami and sweet amino acids in fish samples, while reducing off-flavor generation. The film therefore shows considerable potential as an active packaging material for the preservation of semi-dried fish products.

### 1. Introduction

Low-salt semi-dried fish is a common substitute for traditional salted fish owing to its pleasant taste and unique flavor arising from its low salt and moderate water contents. Chinese consumers generally prefer low-salt semi-dried fish products derived from processed golden pompano; however, the quality of these products is inherently susceptible to degradation due to their high moisture content and nutrient richness. Novel means of improving the quality of golden pompano products, while extending their shelf life during storage, are therefore desirable.

Bio-based coatings and films have attracted significant research attention and have recently been recognized as effective preservation materials that prolong the shelf lives of foodstuffs (Xie et al., 2022). Renewable and edible natural biopolymers, including proteins and polysaccharides, are increasingly favored in food packaging (Zhou et al., 2022). Biopolymers are typically affordable, safe, and environmentally sustainable, rendering them well-suited for food packaging characteristics; they offer the potential to partially replace plastic packaging materials, thereby reducing environmental harm while also enhancing the nutritional value of food (Bhat et al., 2022). Environmentally

sustainable food packaging materials, such as bioactive films, typically incorporate chitosan (CS), an abundant naturally occurring polysaccharide obtained by the deacetylation of chitin, which is commonly found in crustacean and mollusk shells, and fungal cell walls (Xiong et al., 2021). CS possesses excellent film-forming capability and antimicrobial properties; moreover, it is biocompatible and edible (Ashrafi et al., 2018). Furthermore, it can carry a wide range of natural antioxidants that can enhance the synergistic effect of comprehensive preservative systems (Xie et al., 2022).

The hydroxyl groups of polyphenolic active substances present in tea, known as tea polyphenols (TPs), scavenge free radicals, chelate oxidized metal ions, and quench singlet oxygen species, thereby conferring excellent antioxidant activities (Mohajer et al., 2016). TPs are also used as preservatives in a wide range of food storage applications (Zhang et al., 2023). TPs inhibit microbial growth and reproduction, as well as protein and lipid oxidation, retarding the spoilage of aquatic products (Wei et al., 2021); thus, TPs are of particular interest to the aquatic product processing industry. In addition, relative to unmodified CS films, TP-containing CS films exhibit significantly higher radical scavenging rates and antibacterial activities against *Escherichia coli* and

\* Corresponding authors.

E-mail addresses: [heyafu819@163.com](mailto:heyafu819@163.com) (Y. He), [liujing66@hainmc.edu.cn](mailto:liujing66@hainmc.edu.cn) (J. Liu).

<https://doi.org/10.1016/j.fochx.2024.101762>

Received 13 April 2024; Received in revised form 12 August 2024; Accepted 21 August 2024

Available online 23 August 2024

2590-1575/© 2024 The Author(s). Published by Elsevier Ltd. This is an open access article under the CC BY-NC license (<http://creativecommons.org/licenses/by-nc/4.0/>).

*Staphylococcus aureus*. A TP-containing CS film synthesized by Zhou et al. (2022) exhibited good physicochemical properties along with excellent antioxidant and antibacterial activities, thereby extending the shelf life of grass carp.

Furthermore, CS films incorporating TP exhibit significantly higher free radical scavenging rates than unmodified CS films. Additionally, these modified films demonstrate improved antibacterial efficacy against *E. coli* and *S. aureus*. Notably, TP-containing CS films have been shown to effectively extend the shelf life of grass carp owing to their favorable physicochemical properties and exceptional antioxidant and antibacterial properties. Similarly, beef treated with TP-incorporated CS films contained fewer bacterial colonies and less extensive lipid oxidation than that treated with pure CS films (Ashrafi et al., 2018). Despite their advantages, the use of TPs in food applications is limited by their susceptibility to degradation by heat, oxygen, and light during processing and storage, which reduces their stability (Mohajer et al., 2016). Numerous studies have therefore sought to overcome these limitations by improving TP utilization efficiency, and strategies for the development of bio-based nanocarriers based on TP encapsulation have been proposed (Zhang et al., 2024).

As a key component of bone, nano-hydroxyapatite (HAP) is a biological inorganic material with excellent biocompatibility and chemical stability. The porous structure of HAP facilitates the adsorption of active substances (Verma et al., 2023), rendering HAP a potential reinforcing agent for improving the physical properties of natural polymers, including CS, sodium alginate, and collagen; this enables the creation of composite materials with enhanced and desirable characteristics (Deng et al., 2020). For example, the mechanical and barrier properties, and thermal stabilities of collagen fiber films were improved by the addition of HAP (Wang et al., 2016). Moreover, HAP is known to successfully encapsulate various antimicrobial substances within its structure, forming active food packaging systems (Llorens et al., 2012).

In the current study, the effects of the addition of HAP-TP on the structure, physical and mechanical properties, TP release behavior, and antioxidant properties of a CS film are investigated. Additionally, the effects of the resulting CS-HAP-TP composite film on the quality and flavor substances of semi-dried golden pompano during storage are evaluated to provide valuable insights that will aid the future development of new edible bioactive film materials.

## 2. Materials and methods

### 2.1. Materials and chemicals

CS (deacetylation  $\geq 93\%$ , viscosity 100–130 mPa·s, Mw = 15 kDa), glycerol (purity 99%), and the TPs (purity 98%) were purchased from Zhejiang YINO Biotechnology Co., Ltd. (Zhejiang, China). HAP was purchased from EPR Nanomaterials (Nanjing, China). Acetic acid, trichloroacetic acid, anhydrous ethanol, methanol, sodium chloride, barium chloride, and potassium iodide were purchased from Xilong Scientific Co., Ltd. (Guangdong, China). Boric acid, magnesium oxide, forintanol, sodium carbonate, thiobarbituric acid (TBA), sulfosalicylic acid, 2-octanol (GC purity  $>98.0\%$ ), 2,2-biphenyl-1-picrylhydrazyl (DPPH), and 2,2'-biphenylbis (3-ethylbenzothiazoline-6-sulphonic acid) diamine salt (ABTS) were purchased from McLean Biochemistry & Technology (Shanghai, China).

### 2.2. Film preparation

TP (0.4%, w/v) and HAP (1 mg/mL) were added to acetic acid (1% v/v), and the pH of the mixture was adjusted to 4.5 using aqueous NaOH solution (1 M). The mixture was then heated in a water bath at 40 °C for 100 min to afford the HAP-TP complex. These conditions were selected based on optimization experiments (data not shown). CS powder (2% w/v) was then added to the HAP-TP solution before glycerol (30% by mass of CS) was added and the composite solution was ultrasonicated for

30 min. Subsequently, the obtained solution (60 mL) was poured into a 13 × 13 square petri dish and dried at 45 °C for 12 h to form a film, denoted CS-0.1 %HAP-0.4 %TP. CS, CS-0.1 %HAP, CS-0.2 %TP, and CS-0.1 %HAP-0.2 %TP films were obtained using the same method. All dried films were removed from the petri dishes and allowed to stand at 25 °C and 50 % relative humidity (RH) for 48 h to ensure equilibration.

### 2.3. Thickness, color, and opacity determinations

The film thickness was measured at eight random locations over the film using a spiral micrometer to obtain an average value. The film color was determined using a colorimeter, and the total color difference ( $\Delta E$ ) and whiteness index (WI) were calculated using Eqs. (1) and (2), respectively, based on five repeat measurements (Nguyen et al., 2022):

$$\Delta E = \sqrt{(L^* - L)^2 + (a^* - a)^2 + (b^* - b)^2}, \# \quad (1)$$

$$WI = 100 - \sqrt{(100 - L)^2 + (a)^2 + (b)^2}, \# \quad (2)$$

Here, L, a, and b are the color parameters of the films. For reference, the color parameters of a standard whiteboard were  $L^* = 93.87$ ,  $a^* = -0.42$ , and  $b^* = -2.2$ . The absorbance of the film was recorded at 600 nm using an ultraviolet spectrophotometer. The opacity of the film was calculated using Eq. (3):

$$\text{Opacity} = \frac{A_{600}}{X}, \# \quad (3)$$

where  $A_{600}$  is the absorbance of the film at 600 nm, and X is the film thickness (mm).

### 2.4. Measurement of the mechanical properties

Using the method proposed by Yu et al. (2022) with some modifications, the tensile strength (TS, Eq. (4)) and elongation at break (EB, Eq. (5)) of the films were determined using a tensile tester (3343, Instron, MA, USA). The film samples were cut into rectangles (1 cm × 5 cm) with an initial distance of 30 mm. Tensile stretching was performed at a speed of 0.5 mm/s and each sample was tested five times to obtain an average value.

$$TS \text{ (MPa)} = \frac{\text{Force}_{\max} \text{ (N)}}{\text{thickness (m)} \times \text{width (m)}} \# \quad (4)$$

$$EB \text{ (\%)} = \frac{\text{Change in length}}{\text{Initial length}} \times 100. \# \quad (5)$$

### 2.5. Determination of the TP cumulative release rate

The release of TPs from the films was studied using the method proposed by Nguyen et al. (2022) with slight modifications and using ethanol (95% v/v) as the food simulation solution. The films were cut into 80 mm × 80 mm squares and then soaked with the simulation solution (40 mL) in brown bottles. Release tests were then performed in a constant temperature and humidity chamber at 25 °C and 50 % RH. At 100 h intervals, an aliquot of the simulation solution (2 mL) was removed from the bottle, and an aliquot of the blank simulation solution (2 mL) was added to ensure a constant volume, and the test was continued after thoroughly shaking the mixture. The TP concentration was determined using the florinol method, in which the simulation solution (1 mL) was added to a forinol solution (10%, 5 mL) and thoroughly shaken. Subsequently, aqueous NaCO<sub>3</sub> solution (7.5%, 4 mL) was added, and the mixture was allowed to stand for 60 min before its absorbance was measured at 765 nm.

## 2.6. Differential scanning calorimetry

Differential scanning calorimetry (DSC) was performed using a differential scanning calorimeter (Discovery DSC25, TA, Delaware, USA) in reference to Lin et al. (2023). The film (5–6 mg) was heated from 25 to 250 °C in a sealed aluminum pot at a rate of 10 °C/min.

## 2.7. Thermogravimetric analysis

Thermogravimetric analysis (TGA) was performed using a TGA instrument (SDTQ600, TA, Delaware, USA) under flowing nitrogen at a flow rate of 15 mL/min. All samples were heated from 30 to 600 °C.

## 2.8. Fourier transform infrared (FTIR) spectroscopy

The chemical bond characteristics of the prepared films were characterized using Fourier transform-infrared (FT-IR) spectroscopy (Nicolet iS 50 FTIR spectrometer) in the wavelength range of 400–4000 cm<sup>-1</sup>.

## 2.9. Microscopic analysis

The surface and cross-sectional microstructures of the films were observed using scanning electron microscopy (SEM, Gemini Sigma 300, Zeiss). The films were induced to fracture in liquid nitrogen before being immobilized onto conductive adhesive and sprayed with gold for observation.

## 2.10. Water vapor transmission permeability (WVP)

The water vapor permeability (WVP) properties of the films were determined using circular specimens of the films (4.0 cm in diameter). Glass bottles (2.6 cm in diameter) containing distilled water (10 mL) were sealed with the film and weighed at 24 h intervals over a period of 7 d. The WVP properties of the films were calculated using Eq. (6):

$$WVP = \frac{\Delta W \times d}{t \times A \times \Delta p}, \# \quad (6)$$

where  $\Delta W$  is the weight gain of the bottle (g),  $d$  is the thickness of the film (m),  $t$  is the penetration time (s),  $A$  is the area of penetration (m<sup>2</sup>), and  $\Delta p$  is the saturated vapor pressure of pure water at 25 °C.

## 2.11. Oxygen permeation measurements

Oxygen permeation (OP) was measured using the method proposed by Yu et al. (2022) with some modifications. The films were sealed in glass bottles containing a deoxidizer. After recording the initial weights of the bottles, they were placed in a desiccator containing a saturated barium chloride solution (85 % RH) for 48 h. The films were weighed every 24 h for 7 d, and the OP was calculated using Eq. (7):

$$OP = \frac{\Delta m}{t \times A}, \# \quad (7)$$

where  $\Delta m$  is the bottle increment (g),  $t$  is the infiltration time (s), and  $A$  is the infiltration area (m<sup>2</sup>).

## 2.12. Determination of the antioxidant properties

A film specimen (1 g) was shaken in deionized water (50 mL) for 1 h. Subsequently, an aliquot of the resulting solution (2 mL) was mixed homogeneously with DPPH and ABTS solutions (2.5 mL; 0.1 mmol/L) for 30 min, and the absorbance of the mixtures were measured at 517 nm and 734 nm, respectively (Zhou et al., 2022).

## 2.13. Preservation of semi-dried golden pompano by the CS-HAP-TP film

### 2.13.1. Sample processing

A semi-dried golden pompano specimen was prepared according to our previous study (Qiu et al., 2023). Fresh golden pompano was salted in brine (12 % w/v) for 40 min at 4 °C, and then dried at 40 °C for 36 h. Fish samples wrapped in the CS-0.1 %-HAP-0.4 %TP film were denoted the CS-HAP-TP group, while fish samples without film treatment were denoted the control (CON) group. All samples were stored in a thermostatic incubator at 25 °C. Samples were collected on days 0, 7, 14, 28, and 35 to determine the relevant indexes.

### 2.13.2. Determination of pH

The pH was determined using the method proposed by Dai et al. (2022) with slight modifications. A sample (10 g) was added to ultrapure water (100 mL), homogenized and filtered. The pH was measured using a pH meter (PHSJ-5, Jingke, Shanghai, China).

### 2.13.3. Determination of the total viable count (TVC)

Chopped film samples (25 g) were diluted in sterile saline solution (225 mL) and an aliquot (1 mL) of the sample suspension was transferred to an additional saline solution (9 mL) for appropriate dilution. Thereafter, an aliquot (10 µL) of the dilution was added to plate count agar and incubated for 2 d at 37 °C in a thermostat (LRH-70, Yiheng, Shanghai, China).

### 2.13.4. Determination of the total volatile base nitrogen (TVB-N) content

A mashed sample (10 g) was added to distilled water (75 mL) and the mixture was stirred for 30 min. A solution of MgO (5 mL, 10 g/L) was then added to the specimen and the resulting mixture was distilled for 3 min using a Kjeldahl nitrogen apparatus (K9860, Haineng, Shandong, China). Subsequently, the sample was adsorbed using a boric acid solution (30 mL, 20 g/L) containing methyl red and methylene blue indicators and titrated against HCl (0.01 mol/L).

### 2.13.5. Determination of the thiobarbituric acid reactive substances content

The thiobarbituric acid reactive substances (TBARS) content was determined following the method described by Qiu et al. (2023). A sample (5 g) was mixed with a trichloroacetic acid solution (7.5 vol%, 25 mL) and homogenized. The mixture was then centrifuged at 4000 rpm and 4 °C for 10 min and filtered. The filtrate (5 mL) was mixed with a TBA solution (0.02 mol/L, 5 mL), heated at 90 °C for 30 min, and cooled rapidly in an ice-water bath. Finally, the absorbance was measured at 532 nm.

### 2.13.6. Determination of the protein oxidation level

Phosphate-buffered saline (PBS) buffer (pH 7.0) containing EDTA (0.001), NaCl (100 mM), Na<sub>2</sub>HPO<sub>4</sub>/NaH<sub>2</sub>PO<sub>4</sub> (100 mM), MgCl<sub>2</sub> (2 mM) was mixed with each sample in a 4:1 (w/v) ratio and homogenized in an ice-water bath for 1 min. Subsequently, a pellet was obtained by centrifugation for 10 min at 10,000 g and 4 °C, and the supernatant was discarded. The pellet was washed in triplicate with PBS to remove any residual supernatant. PBS containing NaCl (0.06 M) was then added to the resulting precipitate. The mixture was homogenized and extracted statically at 4 °C for 2 h. The supernatant (fish myofibrillar protein (MP)) was then centrifuged at 4 °C for 20 min. The MP sample was analyzed using protein carbonyl content and total sulfhydryl content kits (Jiancheng, Nanjing, China) as per the manufacturer's instructions.

## 2.14. Determination of the free amino acid content

The free amino acid (FAA) content was determined according to the method of Qiu et al. (2023). An automated amino acid analyzer (A300, MembraPure, Germany) was employed with a column incubator temperature ranging from 30 to 70 °C, flow rate of 250 µL/min, injection volume of 20 µL, reactor temperature of 115 °C, and detection

wavelengths of 570 and 440 nm.

### 2.15. Determination of the volatile organic compound content

A sample (6 g) was added to a 15 mL headspace vial, and a solution of 2-octanol (10  $\mu$ L, 100 mg/L) in methanol was added. The sample was extracted by DVB/PDMS using a 65  $\mu$ m extraction head at 55  $^{\circ}$ C for 30 min, followed by thermal desorption at 250  $^{\circ}$ C for 7 min. The chromatographic conditions included an HP-5 MS column (30 m  $\times$  0.25 mm  $\times$  0.25  $\mu$ m) and inlet temperature of 250  $^{\circ}$ C. The initial column temperature of 40  $^{\circ}$ C was maintained for 3 min before heating to 90  $^{\circ}$ C at 5  $^{\circ}$ C/min and maintaining 90  $^{\circ}$ C for 10 min. Further heating to 230  $^{\circ}$ C was performed at a rate of 10  $^{\circ}$ C/min and this temperature was maintained for 7 min. Helium was used as a carrier gas at a flow rate of 0.8 mL/min. The mass spectrometry conditions were as follows: ion source temperature = 230  $^{\circ}$ C; electron ionization (EI) source; electron energy = 70 eV; transmission line temperature = 280  $^{\circ}$ C; quadrupole temperature = 150  $^{\circ}$ C; interface temperature = 250  $^{\circ}$ C; mass scan range = 35–500 amu. The ion fragment peaks fragments were matched with the spectral library in NIST14.0, and then the retention index (RI) of each substance on the HP-5MS column was compared with the RI of the substances identified in the NIST website. The n-alkanes (C7–C24) were measured under the conditions previously described. The RI of unknown compounds was measured using an HP-5MS column with a series of n-alkanes. The volatile organic compound (VOC) content was calculated using Eq. (8):

$$C = \frac{A_v \times m}{A_i \times M} \# \quad (8)$$







where C is the VOC concentration (mg/kg),  $A_v$  is the VOC peak area,  $A_i$  is the area of the 2-octanol peak, m is the weight of 2-octanol ( $\mu$ g), and M is the weight of semi-dried fish (g).

### 2.16. Data analysis

The results of all experiments were expressed as the mean  $\pm$  the standard deviation. Analysis of variance was performed using SPSS version 26.0 software (SPSS Inc., Chicago, USA), and the significance was determined using Duncan's *t*-test, with  $P < 0.05$  being considered as statistically significant.

**Table 1**

Thickness, color opacity and appearance of CS-HAP-TP films.

Sample	Thickness (mm)	L*	a*	b*	$\Delta E$	WI	Opacity	Appearance
No films								
CS	0.069 $\pm$ 0.009a	87.94 $\pm$ 0.71a	-1.34 $\pm$ 0.05d	12 $\pm$ 1.22d	15.42 $\pm$ 1.39d	82.93 $\pm$ 1.34a	5.21 $\pm$ 0.27e	
CS-0.1 %HAP	0.076 $\pm$ 0.004a	89 $\pm$ 1.07a	-1.7 $\pm$ 0.04d	10.08 $\pm$ 1.86e	13.28 $\pm$ 2.08d	84.97 $\pm$ 1.96a	2.86 $\pm$ 0.12d	
CS-0.2 %TP	0.070 $\pm$ 0.007a	67.09 $\pm$ 1.01c	5.55 $\pm$ 0.45b	37.43 $\pm$ 0.72b	48.2 $\pm$ 1.19b	49.85 $\pm$ 1.23b	9.74 $\pm$ 0.22b	
CS-0.1 %HAP-0.2 %TP	0.062 $\pm$ 0.001a	74.5 $\pm$ 1.59b	3.85 $\pm$ 0.37c	30.48 $\pm$ 1.22c	38.24 $\pm$ 1.7c	60.06 $\pm$ 1.78c	8.14 $\pm$ 0.08c	
CS-0.1 %HAP-0.4 %TP	0.072 $\pm$ 0.012a	63.95 $\pm$ 1.72d	12.97 $\pm$ 1.45a	45.93 $\pm$ 0.77a	58.25 $\pm$ 1.79a	40.18 $\pm$ 1.88d	12.52 $\pm$ 0.06a	

## 3. Results and discussion

### 3.1. Thickness, color, and opacity

The thicknesses of the films ranged from 0 to 0.076 mm; however, no significant differences were observed ( $P > 0.05$ ) (Table 1). These results indicate that the addition of HAP and TP had no significant effect on the thickness of the CS films. The smooth and uniform surfaces of the CS films were apparent to the naked eye (Table 1). The total chromatic aberration values ( $\Delta E$ ) of the modified films was significantly higher than that of the CS film, with the exception of the CS-0.1 %HAP film, while the change in the WI showed the opposite trend. This was mainly attributed to the reduction in L and increases in a and b. In addition, the opacity of the HAP-TP-containing films ranged from 8.14 to 12.52, wherein a higher TP concentration significantly increased the film opacity ( $P < 0.05$ ), which was consistent with the appearances of the composite films.

### 3.2. Characterization of the films

#### 3.2.1. SEM

SEM images of the surface and cross-sectional microstructures of the CS, CS-0.1 % HAP, CS-0.2 % TP, CS-0.1 % HAP-0.2 % TP, and CS-0.1 % HAP-0.4 % TP films (Fig. 1) reveal that all five films had uniform surfaces, dense meshes, and were free of cracks. This suggests a high degree of compatibility and strong interactions among CS, HAP, and TP; however, the cross-sectional morphology of the CS composite films was rougher after the addition of HAP, TP, and HAP-TP; moreover, the films with the HAP-TP composite were rougher than those with HAP or TP alone. These results indicate that the HAP-TP complex is uniformly embedded within the CS matrix. This structural change was attributed to tighter cross-linking arising from the interaction between the HAP-TP complex and polymer, which improves the stability of the composite film (Sun et al., 2017).

#### 3.2.2. FTIR spectroscopy

The chemical bonds present in the prepared films were identified using FT-IR spectroscopy. The peak at 3300–3400  $\text{cm}^{-1}$  in the spectra of the films (Fig. 2A) was attributed to O–H/N–H stretching vibrations. This peak was redshifted in the spectra of the CS-0.2 %TP, CS-0.1 %HAP-0.2 %TP, and CS-0.1 %HAP-0.4 %TP films relative to that in the

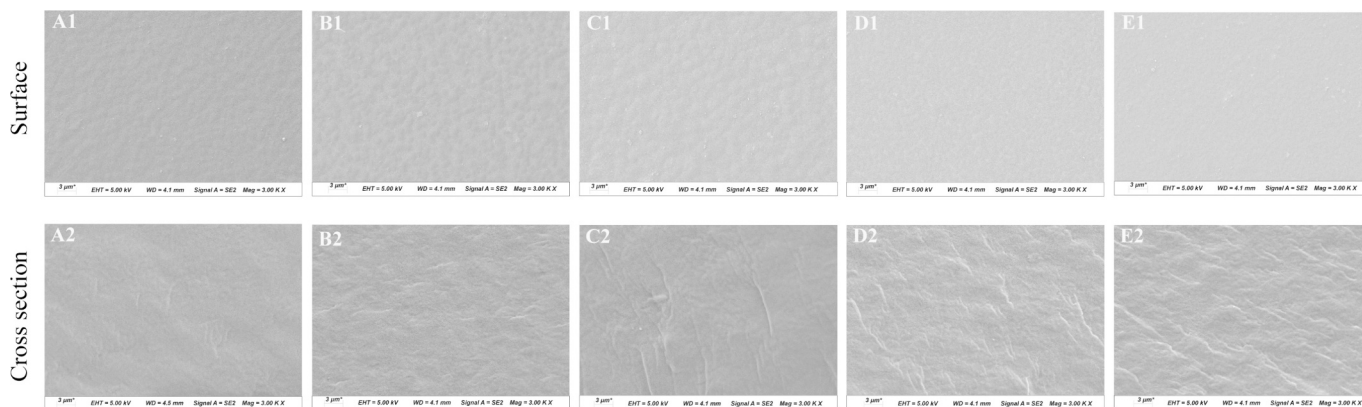


Fig. 1. Surface and cross-sectional SEM images of CS (A), CS-0.1 %HAP (B), CS-0.2 %TP (C), CS-0.1 %HAP-0.2 %TP (D), CS-0.1 %HAP-0.4 %TP (E) films.

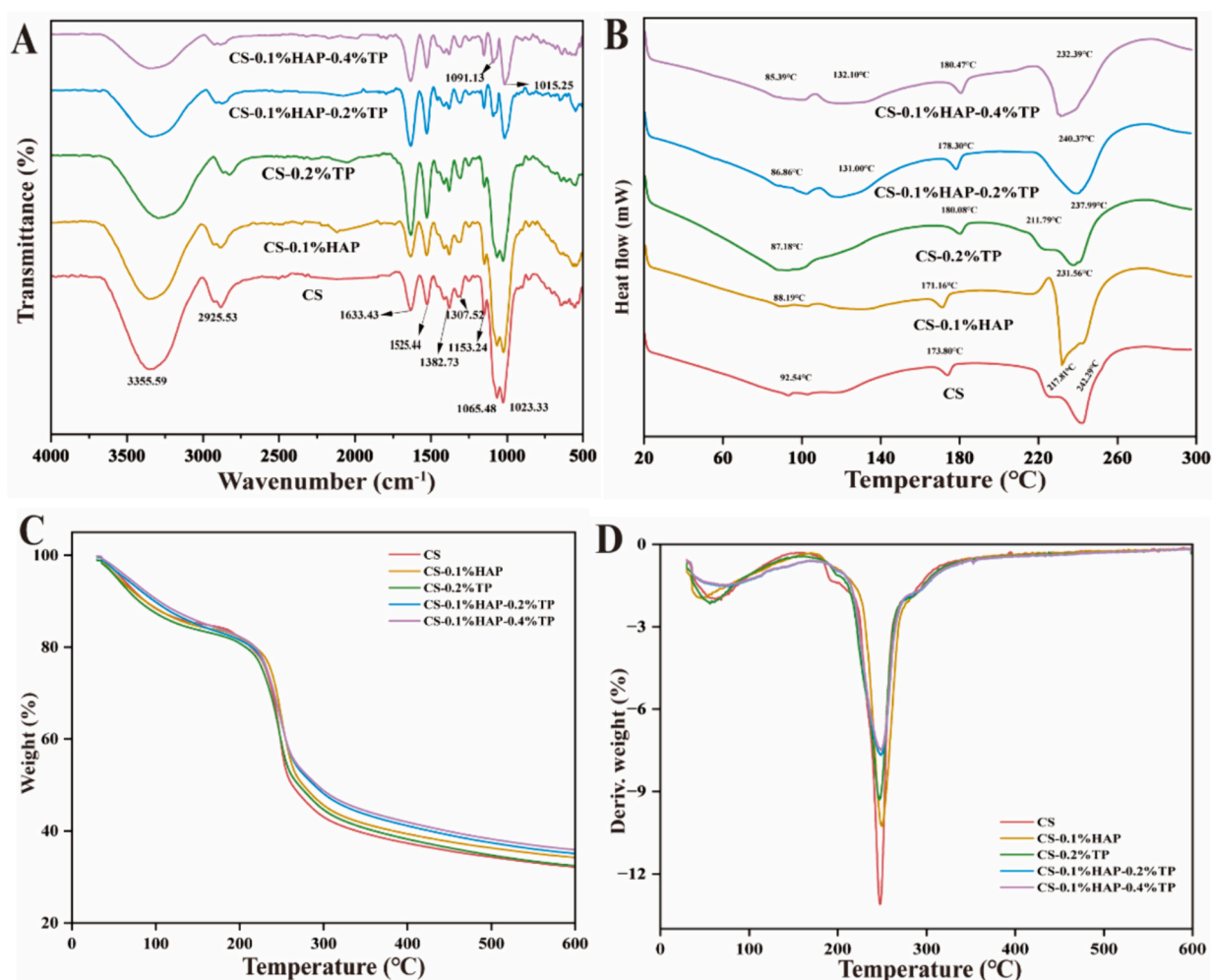


Fig. 2. Fourier transform infrared (FTIR) spectra (A), differential scanning calorimetry (DSC) (B), thermogravimetric analysis (TGA) (C) and derivative thermogravimetric (DTG) analysis (D) of films.

spectrum of the CS film. This shift was attributed to the electrostatic interactions and formation of hydrogen bonds among the CS, TP, and HPA components (Yu et al., 2022). In addition, the peak at 2925.53  $\text{cm}^{-1}$  was attributed to C—H stretching vibrations in the methyl and methylene groups of the film polymer chain. Following addition of the TPs or HAP-TP complex, this peak became less intense ( $P < 0.05$ ). Furthermore, the spectra of the TP-containing films show a significant increase in the intensity of the peaks at 1525.44  $\text{cm}^{-1}$  and 1633.43

$\text{cm}^{-1}$ , which correspond to the amide I (C=O stretching), amide II (N—H bending), and benzene ring stretching vibrations, confirming the successful incorporation of TPs into HAP or CS.

### 3.2.3. DSC

The thermal degradation properties of the films were investigated using DSC. Heat absorption peaks at 85 °C were attributed to water dissipation in all groups, while those at 180 °C were related to the

evaporation of bound water (Fig. 2B). In addition, the peak at 240 °C arises from decomposition of the polymer film (Ma et al., 2019). Notably, water loss from the HAP-TP-containing films required a higher temperature (132 °C), indicating the high thermal stability of the composite films, likely owing to the formation of strong hydrogen bonds between HAP-TP and the CS matrix, which can increase the degrees of crystallinity in the composite film (Ye et al., 2018).

### 3.2.4. TGA

The TGA curves of the various films show two stages of mass loss below 600 °C (Fig. 2C). The first stage of mass loss of 16 % occurred between 30 and 160 °C and was attributed to water evaporation. After complete water evaporation, the second and most significant mass loss occurred between 180 and 350 °C owing to decarboxylation of the CS polymers into carbon oxides and hydrocarbons (Brion-Espinoza et al., 2021). The second stage mass loss from the modified films occurred at higher temperatures than that from the CS film, indicating their superior thermal stability. The maximum thermal decomposition temperature of all films was 250 °C. Additionally, the most pronounced peak was observed in the derivative thermogravimetric curve of the CS film (Fig. 2D), further confirming the higher degradation temperatures and thermal stabilities of the modified films, which may be explained by the superior heat resistance properties of the TP- HAP complex. The residual weight ratios of all films increased slightly at 600 °C in the presence of TPs or HAP, reaching 32.45 % (CS-TP film), 34.25 % (CS-HAP film), and 35.12 and 35.94 % (CS-HAP-TP films), which are higher than that of the CS film (32.18 %). These results indicate that the incorporation of the HAP-TP composite endowed the CS film with superior thermal stability, likely owing to strong interactions between the complex and the film matrix, as indicated by the FTIR spectra.

### 3.3. Mechanical properties of the films

Food packaging films require a balance of flexibility and strength; thus, a comparative analysis of the TS and EB characteristics of the various films was conducted. The TS and EB values of the CS film were 16.70 MPa and 28.92 %, respectively. The TS value increased upon adding the TPs or HAP, with the CS-0.1 %HAP-0.4 %TP film having the highest TS of 126.23 %, an increase of 48.54 % (Fig. 3A). This difference was attributed to the potential ability of the HAP particles to reinforce the film substrate and undergo rigid blending with the TPs. The large surface area of HAP also facilitates its dispersion in and compatibility with the film, while physical entanglement between HAP-TP and the CS polymer networks form a homogeneous film matrix, thereby increasing the TS (Shemshad et al., 2018). Similarly, the addition of TPs and HAP significantly increased the EB values of the films ( $P < 0.05$ ), with the CS-0.1 %HAP-0.4 %TP film demonstrating the highest increase of 67.87 % (Fig. 3B). This may be attributed to the enhanced migratory properties of the molecular chains in the film (Vijayakumar et al., 2022). Moreover, in the presence of HAP, the TS and EB values of the composite films tended to increase with the TP content.

### 3.4. Barrier properties of the films

#### 3.4.1. WVP

The addition of TPs, either alone or in combination with HAP, had a significant effect ( $P < 0.05$ ) on the WVP of the tested films. The WVP of the films in the CS and CS-0.1 %HAP-0.4 %TP groups were  $7.69 \times 10^{-10}$  g/ms•Pa and  $5.40 \times 10^{-10}$  g/ms•Pa, respectively; thus, modifying the films with HAP and TP reduced the WVP by 29.78 % (Fig. 3C). This result indicates that the addition of TPs and HAP effectively improved the water barrier properties of the films. This effect was attributed to reduced water migration owing to an increase in the number of intermolecular hydrogen bonds and a reduction in the number of free hydroxyl groups. The HAP-TP composite filled the cavities between the polymer chains, creating a longer water transport pathway (Zhang et al.,

2022), and increasing the probability of inhibiting or preventing penetration.

#### 3.4.2. OP

The OP describes the ability of oxygen to pass through a film. The OP values of all composite films developed in this study were lower than those of CS film ( $P < 0.05$ ; Fig. 3D), suggesting that the addition of TPs or HAP facilitates the formation of an effective oxygen barrier. In particular, the OP of the CS-0.1 %HAP-0.4 %TP was 35.59 % lower than that of the CS film, having the lowest OP of the various films evaluated in this study ( $1.14 \times 10^{-3}$  g/ms). This reduction was attributed to dispersion of the HAP-TP composite within the film matrix and the formation of hydrogen bonds among these components to create a dense structure with lower oxygen diffusion (Bhat et al., 2022).

### 3.5. TP release properties of the films

The TP release behavior was studied for 700 h at 25 °C using 95 % ethanol as a fat food simulant (Fig. 3E). The cumulative TP release rate of CS-0.1 %HAP-0.2 %TP film was 6.79 % lower than that of the CS-0.2 %TP film after 700 h; moreover, the TP release rate was well controlled in the former case. The amount of TP released from the CS-0.1 %HAP-0.2 %TP initially increased significantly over time, reaching a relative plateau after 600 h. In previous studies (Liu et al., 2017), the initial rapid release of TP was considered to provide short-term protection, while the subsequent slower release ensured medium/long-term protection. TP was rapidly released from the CS-0.2 %TP film owing to its unbound nature within the CS structure; the slower release of TP from the CS-0.1 %HAP-0.2 %TP and CS-0.1 %HAP-0.4 %TP films were attributed to the longer diffusion pathways formed by HAP encapsulation. These latter two groups therefore exhibited lower cumulative release rates. The TP release rate also increased with the TP content, likely owing to the higher concentration of free TP in these structures. At 700 h, the CS-0.1 %HAP-0.2 %TP and CS-0.1 %HAP-0.4 %TP films showed cumulated TP release rates of 43.13 % and 46.43 %, respectively. These results indicate that incorporation of the HAP-TP complex enables the slow release of TP, thereby improving its stability and prolonging the antioxidant activity of the film.

### 3.6. Antioxidant activities of the films

The antioxidant properties of the films were evaluated using DPPH and ABTS free radical scavenging assays (Fig. 2F and G). The incorporation of TPs and HAP-TP into the CS films significantly enhanced their free radical scavenging capability ( $P < 0.05$ ). In addition, the DPPH and ABTS radical scavenging capacity of the CS-0.1 %HAP-0.2 %TP film was significantly lower ( $P < 0.05$ ) than that of the CS-0.2 %TP films, suggesting that the encapsulation of TP by HAP enabled the controlled release of TP and maintained a stronger antioxidant activity over a longer time. In contrast, the DPPH and ABTS radical scavenging capacity of the CS-0.1 %HAP-0.4 %TP film was significantly higher ( $P < 0.05$ ) than that of the CS-0.1 %HAP-0.2 %TP film, being similar to that of the CS-0.2 %TP film. Polyphenols are known to scavenge free radicals by transferring hydrogen atoms from the reactive hydroxyl groups to the DPPH and ABTS free radicals; thus, the position and total number of hydroxyl groups in a polyphenol largely determine its antioxidant activity (Huang et al., 2023).

### 3.7. Use of the CS-HAP-TP film in preserving semi-dried golden pompanos

#### 3.7.1. TVC

Fish spoilage is primarily caused by microbial proliferation. High microbial proliferation was observed in the CON group following storage of the semi-dried golden pompano sample for 28 d, with TVC reaching 7.47 log CFU/g. In contrast, the TVC of the CS-HAP-TP film-treated group was significantly lower (6.53 log CFU/g,  $P < 0.05$ ,

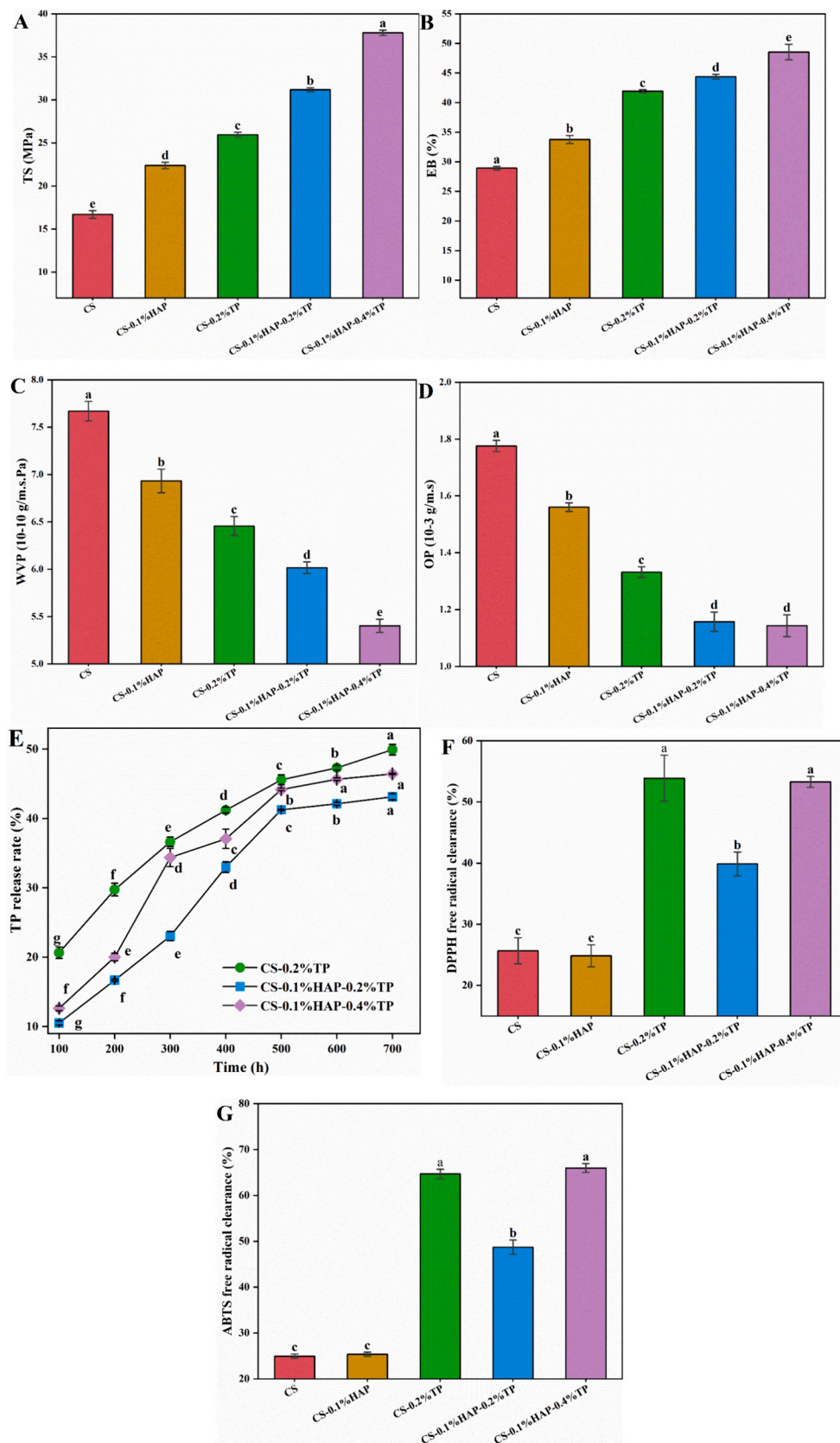


**Fig. 3.** Properties of CS-HAP-TP films: Tensile strength (TS) (A), elongation at break (EB) (B), water vapor permeation (WVP) (C), oxygen permeation (OP) (D), cumulative release rate of TP in food simulants (E), and scavenging of free radicals by DPPH (F) and ABTS (G). The different lower-case letters indicate statistically significant differences between different samples ( $P < 0.05$ ).

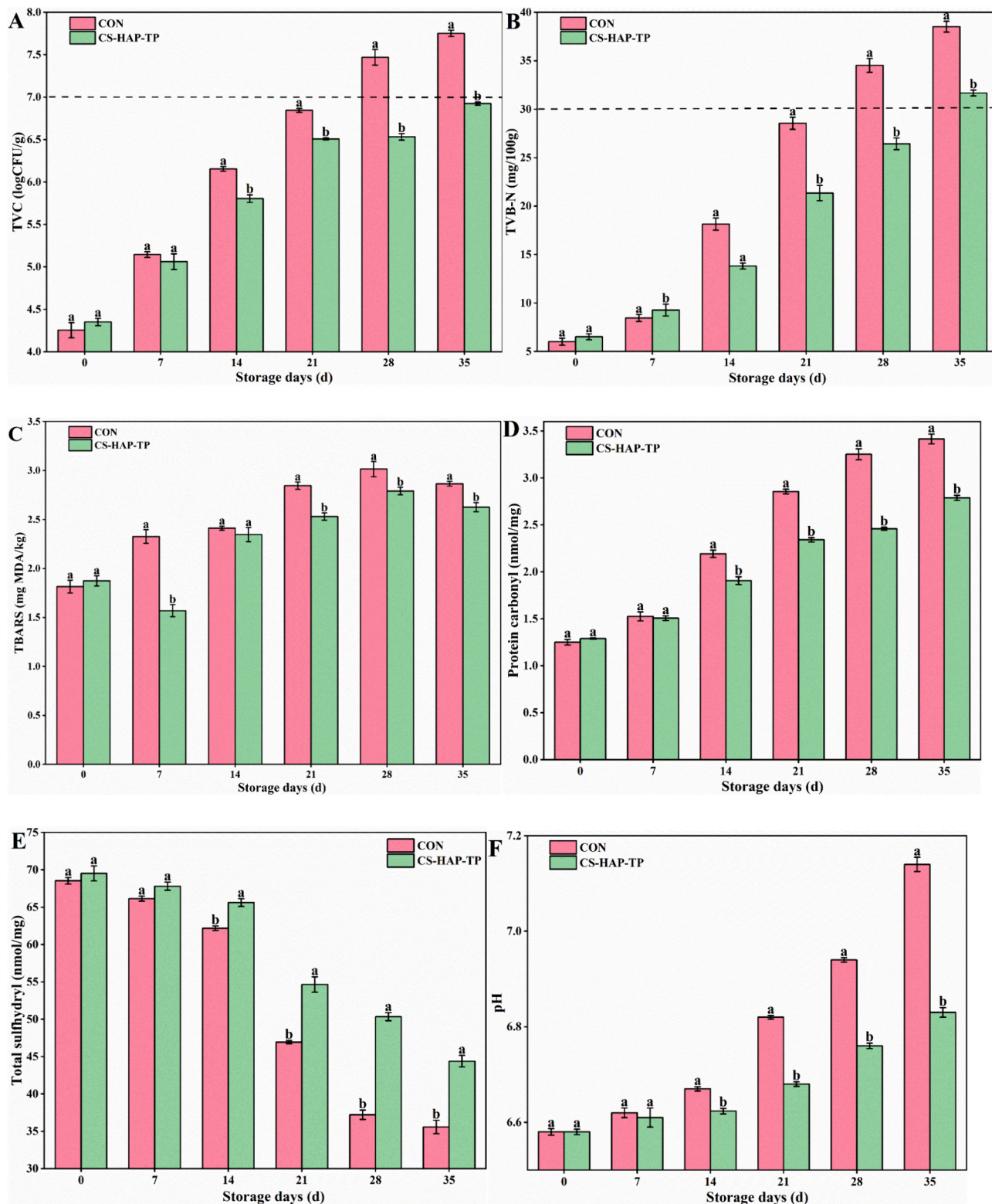


**Fig. 4.** Total viable count (TVC) (A), total volatile base nitrogen (TVB-N) (B), thiobarbituric acid reactive substances (TBARS) (C), protein carbonyls (D), total sulfhydryl groups (E), and pH (F) of semi-dried golden pompano in the control and coated groups during storage. The different lowercase letters indicate statistically significant differences between different samples ( $P < 0.05$ ).

Fig. 4A), and is lower than the upper limit of 7 log CFU/g allowed in edible fish (Wu et al., 2016). This reduction in TVC was attributed to the antimicrobial effects of CS and TP, along with the excellent barrier properties of the prepared film (Liu et al., 2021). The antibacterial effects of TP and CS can be attributed to the inhibition of DNA and RNA

synthesis, reduction in bacterial enzyme activity and energy metabolism, and bacterial death (Houicher et al., 2021; Siripatrawan & Vitchayakitti, 2016). The prepared films effectively inhibited microbial growth and extended the edible shelf life of dried golden pompano by >7 d.



### 3.7.2. TVB-N content

The TVB-N compounds produced by protein degradation are important markers of fish quality and deterioration. Thus, the TVB-N contents of the various treatment groups were evaluated after storage for 7 d, wherein a similar trend was observed to that of the TVC. The TVB-N content was significantly lower ( $P < 0.05$ ) in the CS-HAP-TP groups (Fig. 4B), suggesting that the inhibition of microbial growth is an important factor for reducing the TVB-N content. At 28 d of storage, the TVB-N contents of the CON and CS-HAP-TP groups were 34.52 and 26.43 mg/100 g, respectively; notably, a TVB-N content of 30 mg/100 g is an indicator of spoilage (Wu et al., 2016). These results confirm that the CS-HAP-TP film preserved the semi-dried golden pompano during ambient storage, likely owing to the antimicrobial and anti-endogenous enzyme activity of the TPs, which inhibit proteolysis (Wu et al., 2016).

### 3.7.3. Lipid oxidation

Fig. 3C shows the changes in TBARS content of the film-encapsulated semi-dried golden pompano fish samples over 35 d of storage. After 14 d, the TBARS content of the CS-HAP-TP group was significantly lower than that of the CON group ( $P < 0.05$ ). This was attributed to the antioxidant properties of chitosan and TP, which inhibited lipid oxidation to some extent. These results suggest that wrapping the fish samples with the CS-HAP-TP film effectively retards lipid oxidation during storage.

### 3.7.4. Protein oxidation

The degree of protein oxidation during storage for 35 d was evaluated based on the carbonyl and total sulfhydryl contents. Treatment with CS-HAP-TP films significantly reduced the carbonyl content ( $P < 0.05$ ) relative to that of the CON group (Fig. 4D), likely because the CS-HAP-TP film blocked the entry of oxygen and water vapor to a certain extent, thereby inhibiting protein oxidation in the semi-dried golden pompano specimen. Furthermore, the total sulfhydryl content of the CON group significantly decreased from 68.55 to 35.57 nmol/mg during the ambient storage period, while that of the CS-HAP-TP group on day 35 was 44.38 nmol/mg ( $P < 0.05$ ; Fig. 4E). These results indicate that CS-HAP-TP treatment scavenges free radicals and thus prevents oxidation of the sulfhydryl groups, which effectively inhibits protein oxidation and prevents the fish from spoiling (Xiong et al., 2021).

### 3.7.5. pH

The pH of a fish sample is known to affect its shelf life; thus, we evaluated the pH values of the various semi-dried golden pompano treatment groups. Over time, the pH of the samples increased, with the pH of the CON group being higher than that of the CS-HAP-TP group throughout the storage period (Fig. 4F). This was attributed to the accumulation of TVB-N substances produced by microbial proliferation. Thus, the antioxidant and antimicrobial properties imparted by the CS-HAP-TP film inhibited the accumulation of TVB-N compounds (Fig. 4B),

thereby slowing the pH increase. These results indicate that the CS-HAP-TP film inhibited the deterioration of the semi-dried golden pompano sample.

### 3.8. FAA content

FAAs are of vital importance to the flavor attributes of aquatic products and can indicate the nutritional value and freshness of such products (Leggio et al., 2012). In this study, 15 major FAAs in the CON and film-treated semi-dried golden pompano samples were quantified and changes in the FAA contents during storage were visualized using a clustered heat map. Fig. 5A shows the FAA concentrations in the CON and CS-HAP-TP groups at days 0, 14 and 35, wherein higher concentrations of lysine (Lys), glutamic acid (Glu), alanine (Ala), glycine (Gly), and leucine (Leu) are clustered on the right side, while lower levels of tyrosine (Tyr), aspartic acid (Asp), serine (Ser), and arginine (Arg) are clustered on the left side. The thermogram shows that the contents of many FAAs increased significantly ( $P < 0.05$ ) after 14 d in storage. Notably, the FAAs present in the fish specimens are mainly derived from protein and peptide hydrolysis, which is catalyzed by the extracellular proteases of spoilage bacteria (Lou et al., 2021). Fig. 4B shows the changes in the contents of bitter amino acids, sweet amino acids (SAAs), and umami amino acid (UAAs) in the semi-dried golden pompano samples during storage. The formation of bitter FAAs (e.g., Leu, isoleucine (Ile), and histidine (His)) in the fish meat was significantly inhibited in the CS-HAP-TP group relative to the CON group (Fig. 5B and Table S1). The UAA (Asp and Glu) and SAA (Thr, Ser, Gly, Ala, Lys, Val, and Met) contents are known to contribute to the desirable flavor of this fish, and notably, these FAAs collectively accounted for 77.76 % of the total FAAs in the samples. In the later stages of storage, the contents of these amino acids decreased significantly ( $P < 0.05$ ), indicating a deterioration in the flavors of the samples. In addition, ammonia, amines, aldehydes, alcohols, and acids were produced via deamination reactions, resulting in an unpleasant fishy flavor. The decomposition of some amino acids also produced histamine, cadaverine, and putrescine, which produced pungent flavors (Cheng et al., 2023). The UAA and SAA contents of the CS-HAP-TP group increased by 17.25 and 14.14 %, respectively, compared with those of the CON group after storage for 35 d, indicating a significant inhibition of the oxidative degradation of FAAs. These results were attributed to the potential antioxidant effect of the film, and suggest that application of the CS-HAP-TP film maintains the fresh and sweet flavor of semi-dried golden pompano.

### 3.9. VOC levels

This study identified a total of 77 VOCs in the semi-dried golden pompano fish sample during ambient storage, including 7 ketones, 11 aldehydes, 11 alcohols, 7 acids, 8 esters, 4 amines, 17 alkanes, 9 olefins,

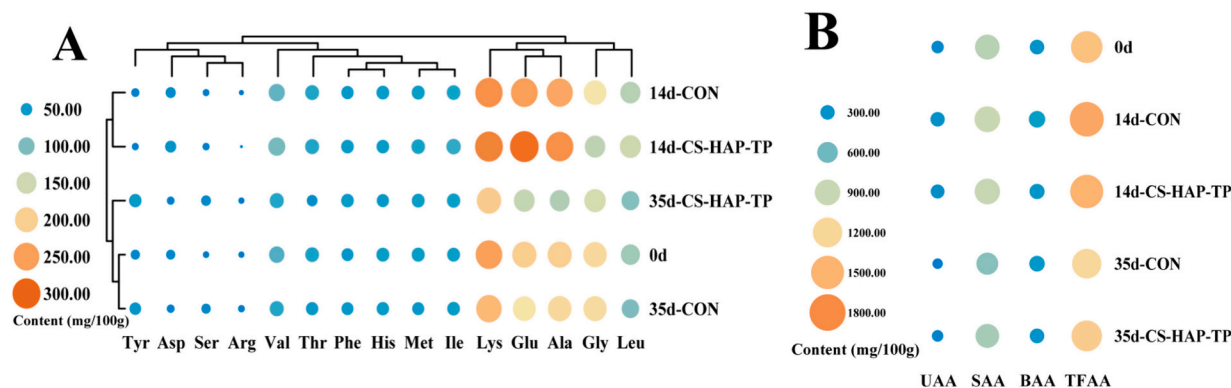
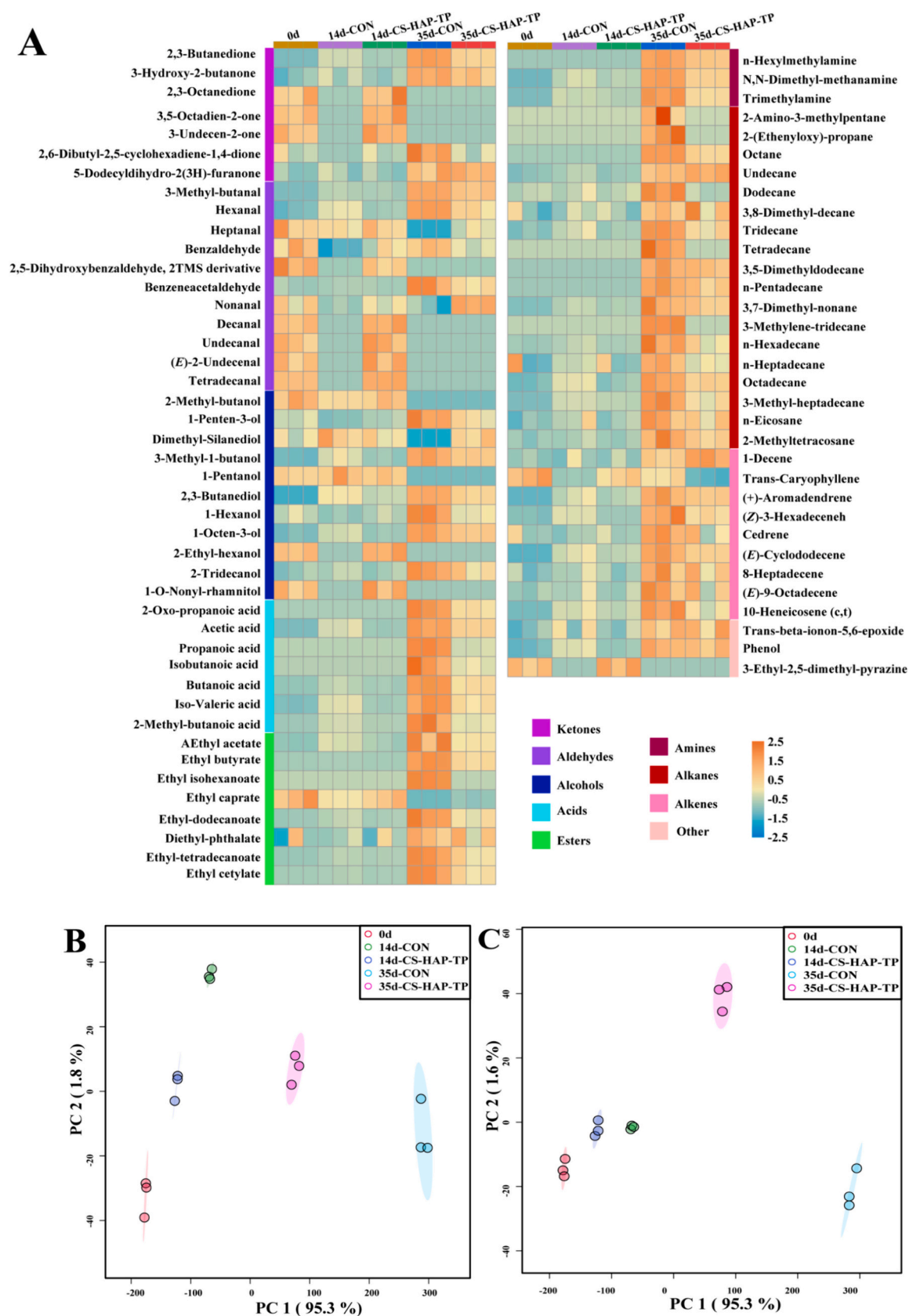


Fig. 5. Cluster analysis plot (A) and species variation (B) of FAA during ambient storage of semi-dried golden pomfret in control and wrapped groups. UAA: umami amino acid, SAA: sweet amino acid, BAA: bitter amino acid, TFAA: total free amino acid.



**Fig. 6.** Thermograms (A), PCA (B) and PLS-DA (C), VIP score (D) and categorical bar graphs (E) of volatile organic compounds (VOCs) of semi-dried golden pompano fish in control and wrapped groups during storage. A: The color of each square in different rows indicate the relative concentration of VOCs in different samples. Red squares indicate higher levels of VOC, whereas blue squares indicate lower levels of VOC. (For interpretation of the references to color in this figure legend, the reader is referred to the web version of this article.)

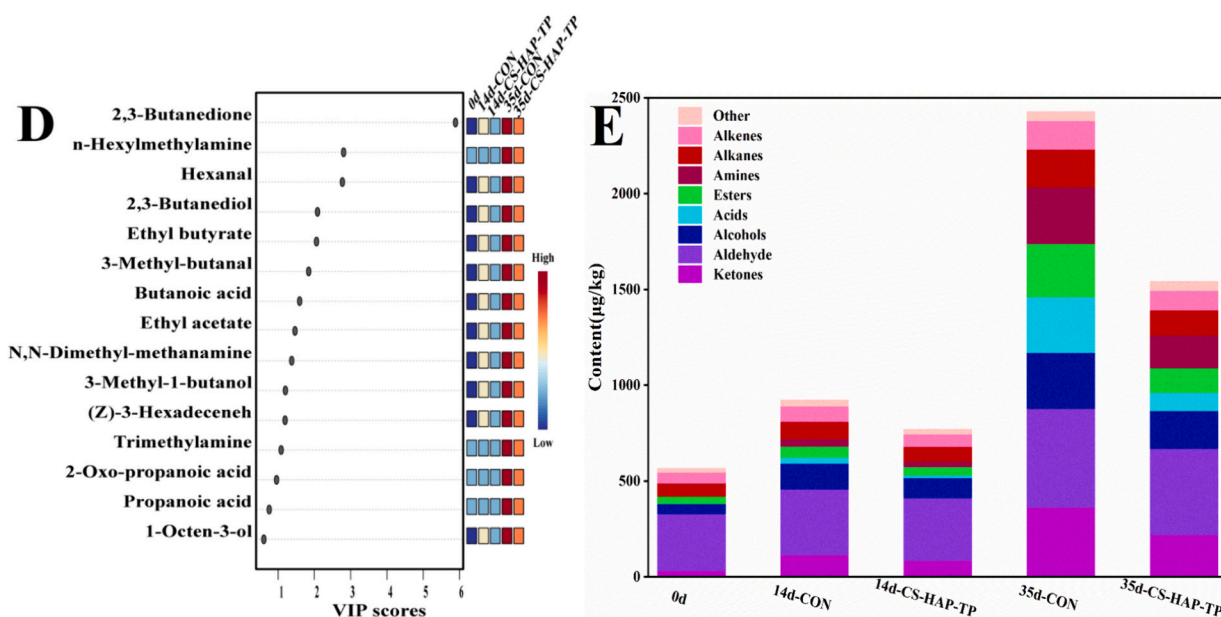


Fig. 6. (continued).

and 3 other compounds (Fig. 6A and Table S2). The hydrocarbons were the most diverse group of VOCs, while the aldehydes were the most concentrated. During storage, the total concentrations of all VOCs increased significantly ( $P < 0.05$ ), likely owing to the effects of microbial metabolism and lipid/protein oxidation, which are known to produce various VOCs. The production of such compounds gives fish an undesirable flavor and ultimately reduces edibility (Fidalgo et al., 2021). The VOC concentrations increased throughout the storage period (Fig. 6), although lower levels were observed in the CS-HAP-TP group (c. f., the CON group; Fig. 6A). This result demonstrates the inhibitory effect of the CS-HAP-TP coating on the production of undesirable flavor substances in semi-dried golden pompano during ambient storage.

The differences in the VOC contents of the various samples was elucidated by principal component analysis, and the cumulative contribution from all samples was determined to be 97.2 % (PC1: 95.3 %, PC2: 1.8 %; Fig. 6B). This result suggests that the semi-dried golden pompano samples were better differentiated in the fractional plot. Notably, significant differences were observed in the VOC contents of the samples after 0, 14, and 35 d, with particularly significant differences between the fresh samples (low levels) and those at the end of the storage period (high levels). Additionally, the VOC levels of the CS-HAP-TP and CON groups differed significantly ( $P < 0.05$ ). Furthermore, the difference between the CS-HAP-TP group and the fresh sample was less significant than that between the CON group and the fresh samples after 35 d, suggesting that the CS-HAP-TP film facilitates the retention of natural VOCs during the ambient storage of semi-dried golden pompano.

The variable importance in projection (VIP) coefficient was calculated using the PLS-DA model (Fig. 6C) to explore the contributions of the various VOCs to sample differentiation, wherein a VIP  $\geq 1$  indicates a crucial factor in the differentiation process. Twelve potential VOC markers were screened for VIP coefficients  $>1$  (Fig. 6D), of which 2,3-butanedione, *n*-hexylmethylamine, hexanal, 2,3-butanediol, ethyl butyrate, 3-methyl-butanal, and butanoic acid were the major volatile components affecting the flavor of the semi-dried golden pompano samples. Observational screening showed that aldehydes were the most abundant VOCs, followed by ketones, amines, and alcohols.

Aldehydes are common degradation products of lipid oxidation and amino acid catabolic reactions that are known to contribute significantly to the flavor of semi-dried fish owing to their low aroma thresholds (Peinado et al., 2016). The oxidative rancidity of marine fish rich in unsaturated fatty acids is primarily attributed to aldehydes, markers of

which include 3-methyl-butanal and hexanal, wherein the former may originate from the deamination of Leu. This compound is produced via a Strecker degradation reaction and causes a foul odor due to its low odor threshold (Casaburi et al., 2015). The total aldehyde concentration of the CS-HAP-TP-treated sample was significantly lower than that of the CON group at the end of storage ( $P < 0.05$ , Fig. 6E), indicating that lipid oxidation and protein degradation were effectively inhibited in the CS-HAP-TP group owing to the antioxidant and radical-scavenging effects imparted by the film (Dai et al., 2022).

Ketones are mainly produced by lipid autoxidation or via the Strecker degradation of amino acids, and are associated with various off-flavors (Peinado et al., 2016) despite having a less pronounced influence than aldehydes in determining the sample flavor. Among the ketones identified in this study, the concentrations of 2,3-octanediol, 3,5-octadien-2-one, and 3-undecen-2-one decreased significantly ( $P < 0.05$ ) during storage, whereas those of 2,3-butanedione and 3-hydroxy-2-butanone significantly increased (Fig. 6A). 3-hydroxy-2-butanone may be formed by the oxidation of oleic acid and the glucose catabolism of spoilage microbes (Casaburi et al., 2015).

Finally, alcohols are mainly produced via lipid oxidation, microbial action, and the metabolism of amino acids. Lipid oxidation generally affords straight-chain alcohols, while microbial action forms most branched-chain alcohols through the degradation of branched-chain aldehydes (Liu et al., 2023). The most abundant alcohols detected in this study were 3-methyl-1-butanol, 2,3-butanediol, and 1-octen-3-ol (Fig. 6A). 3-Methyl-1-butanol is produced by the degradation of 3-methyl-butanal, which in turn is derived from Leu and by the action of aldehyde reductase. In addition, 2,3-butanediol has a buttery flavor and is synthesized by the reduction of acetoin by bacteria during the pyruvate metabolic pathway (Casaburi et al., 2015). 1-Octen-3-ol is produced by the action of lipoxigenase on *n*-3 and *n*-6 polyunsaturated fatty acids and by the auto-oxidation of linoleic acid (Fratini et al., 2012); it can produce off-flavors, such as a mushroom-like odor, owing to its low odor threshold. The alcohol content of the CS-HAP-TP group was significantly reduced during storage relative to that of the CON group. This difference may be related to the inactivation of lipoxigenase by the interaction of phenolic compounds with the sulfhydryl groups in proteins. Notably, the antimicrobial properties of CS also helped lower the alcohol content (Cowan, 1999; Siripatrawan & Vitchayakitti, 2016).

#### 4. Conclusion

A HAP-TP complex was added to CS film. The mechanical properties and thermal stability of the film were improved by intermolecular interactions and hydrogen bonding between the HAP-TP complex and the CS film matrix, with the tensile strength and elongation at break increasing by 126.22 and 67.87 %, respectively. The addition of HAP-TP also increased the density of the films, thereby reducing their water vapor transmission and optical permeability by 29.78 and 35.59 %, respectively. Furthermore, the cumulative release of the CS-HAP-TP film was reduced by 6.79 % at 700 h relative to that of the CS film, while the DPPH radical scavenging ability was significantly higher in the former case, suggesting that the composite CS-HAP-TP film enabled the controlled release of TP and thus prolonged its antioxidant effect. Moreover, the application of this film significantly inhibited the oxidation of both lipids and proteins of semi-dried fish during storage, and significantly delayed increases in the microbial proliferation and TVB-N. Consequently, the film prolonged the shelf life of the product by >7 d relative to the control group ( $P < 0.05$ ). Furthermore, the film wrapping effectively prevented the loss of umami and sweet amino acids, while inhibiting the formation of off-flavor VOCs during storage. This CS-HAP-TP film demonstrates excellent performance in the preservation of semi-dried golden pompano.

#### Funding

This study was supported by a Key Research and Development Project fund from Hainan Province [ZDYF2024XDNY258], an International Scientific and Technological Cooperation R&D project fund from Hainan Province [GHYF2024022], a Science and Technology Plan Project grant from Haikou [2022-020], a Collaborative Innovation Center Project grant from Hainan University [XTCX2022HYC10], and the Education Department of Hainan Province [Hnky2024-31].

#### CRedit authorship contribution statement

**Dan Qiu:** Writing – original draft, Investigation, Data curation. **Jingxuan Zhou:** Investigation, Formal analysis. **Qiaohui Feng:** Investigation, Formal analysis. **Kun Ren:** Methodology. **Hongying Zhang:** Conceptualization. **Yanfu He:** Writing – review & editing, Supervision, Formal analysis. **Chuan Li:** Visualization, Resources. **Jing Liu:** Supervision, Methodology. **Nga Thi Tuyet Mai:** Resources, Conceptualization.

#### Declaration of competing interest

The authors declare that they have no known competing financial interests or personal relationships that could have appeared to influence the work reported in this paper.

#### Data availability

The authors do not have permission to share data.

#### Appendix A. Supplementary data

Supplementary data to this article can be found online at <https://doi.org/10.1016/j.fochx.2024.101762>.

#### References

- Ashrafi, A., Jokar, M., & Mohammadi Nafchi, A. (2018). Preparation and characterization of biocomposite film based on chitosan and kombucha tea as active food packaging. *International Journal of Biological Macromolecules*, 108, 444–454. <https://doi.org/10.1016/j.ijbiomac.2017.12.028>
- Bhat, V. G., Narasagoudar, S. S., Masti, S. P., Chougale, R. B., Vantamuri, A. B., & Kasai, D. (2022). Development and evaluation of Moringa extract incorporated chitosan/guar

- gum/poly (vinyl alcohol) active films for food packaging applications. *International Journal of Biological Macromolecules*, 200, 50–60. <https://doi.org/10.1016/j.ijbiomac.2021.12.116>
- Brion-Espinoza, I. A., Iniguez-Moreno, M., Ragazzo-Sánchez, J. A., Barros-Castillo, J. C., Calderón-Chiu, C., & Calderón-Santoyo, M. (2021). Edible pectin film added with peptides from jackfruit leaves obtained by high-hydrostatic pressure and pepsin hydrolysis. *Food Chemistry: X*, 12, Article 100170. <https://doi.org/10.1016/j.fochx.2021.100170>
- Casaburi, A., Piombino, P., Nychas, G.-J., Villani, F., & Ercolini, D. (2015). Bacterial populations and the volatilome associated to meat spoilage. *Food Microbiology*, 45, 83–102. <https://doi.org/10.1016/j.fm.2014.02.002>
- Cheng, H., Wang, J., & Xie, J. (2023). Progress on odor deterioration of aquatic products: Characteristic volatile compounds, analysis methods, and formation mechanisms. *Food Bioscience*, 53, Article 102666. <https://doi.org/10.1016/j.fbio.2023.102666>
- Cowan, M. M. (1999). Plant products as antimicrobial agents. *Clinical Microbiology Reviews*, 12(4), 564–582.
- Dai, W., Yan, C., Ding, Y., Wang, W., Gu, S., Xu, Z., & Ding, Y. (2022). Effect of a chitosan coating incorporating epigallocatechin gallate on the quality and shelf life of bighead carp (*Aristichthys nobilis*) fillets during chilled storage. *International Journal of Biological Macromolecules*, 219, 1272–1283.
- Deng, L., Li, Y., Zhang, A., & Zhang, H. (2020). Characterization and physical properties of electrospun gelatin nanofibrous films by incorporation of nano-hydroxyapatite. *Food Hydrocolloids*, 103. <https://doi.org/10.1016/j.foodhyd.2019.105640>
- Fidalgo, L. G., Simões, M. M. Q., Casal, S., Lopes-da-Silva, J. A., Delgadillo, I., & Saraiva, J. A. (2021). Enhanced preservation of vacuum-packaged Atlantic salmon by hyperbaric storage at room temperature versus refrigeration. *Scientific Reports*, 11(1), 1668. <https://doi.org/10.1038/s41598-021-81047-4>
- Fratini, G., Lois, S., Pazos, M., Parisi, G., & Medina, I. (2012). Volatile profile of Atlantic shellfish species by HS-SPME GC/MS. *Food Research International*, 48(2), 856–865. <https://doi.org/10.1016/j.foodres.2012.06.033>
- Houicher, A., Bensed, A., Regenstein, J. M., & Özogul, F. (2021). Control of biogenic amine production and bacterial growth in fish and seafood products using phytochemicals as biopreservatives: A review. *Food Bioscience*, 39, Article 100807. <https://doi.org/10.1016/j.fbio.2020.100807>
- Huang, Z., Wang, Q., Cao, J., Zhou, D., & Li, C. (2023). Mechanisms of polyphenols on quality control of aquatic products in storage: A review. *Critical Reviews in Food Science and Nutrition*, 1–20. <https://doi.org/10.1080/10408398.2023.2167803>
- Leggio, A., Belsito, E. L., De Marco, R., Liguori, A., Siciliano, C., & Spinella, M. (2012). Simultaneous extraction and derivatization of amino acids and free fatty acids in meat products. *Journal of Chromatography A*, 1241, 96–102. <https://doi.org/10.1016/j.chroma.2012.04.029>
- Lin, X., Chen, S., Wang, R., Li, C., & Wang, L. (2023). Fabrication, characterization and biological properties of pectin and/or chitosan-based films incorporated with noni (*Morinda citrifolia*) fruit extract. *Food Hydrocolloids*, 134, Article 108025. <https://doi.org/10.1016/j.foodhyd.2022.108025>
- Liu, F., Avena-Bustillos, R. J., Chiou, B.-S., Li, Y., Ma, Y., Williams, T. G., & Zhong, F. (2017). Controlled-release of tea polyphenol from gelatin films incorporated with different ratios of free/nanoencapsulated tea polyphenols into fatty food simulants. *Food Hydrocolloids*, 62, 212–221. <https://doi.org/10.1016/j.foodhyd.2016.08.004>
- Liu, J., Shao, Y., Yuan, C., Takaki, K., Li, Y., Ying, Y., & Hu, Y. (2021). Eugenol-chitosan nanoemulsion as an edible coating: Its impact on physicochemical, microbiological and sensorial properties of hairtail (*Trichiurus haumela*) during storage at 4 °C. *International Journal of Biological Macromolecules*, 183, 2199–2204. <https://doi.org/10.1016/j.ijbiomac.2021.05.183>
- Liu, K., Yang, P., Zhang, X., Zhang, D., Wu, L., Zhang, L., & Rong, L. (2023). Metabolic cross-feeding enhances branched-chain aldehydes production in a synthetic community of fermented sausages. *International Journal of Food Microbiology*, 407, Article 110373. <https://doi.org/10.1016/j.ijfoodmicro.2023.110373>
- Llorens, A., Lloret, E., Picouet, P. A., Trbojevič, R., & Fernandez, A. (2012). Metallic-based micro and nanocomposites in food contact materials and active food packaging. *Trends in Food Science & Technology*, 24(1), 19–29. <https://doi.org/10.1016/j.tifs.2011.10.001>
- Lou, X., Zhai, D., & Yang, H. (2021). Changes of metabolite profiles of fish models inoculated with *Shewanella baltica* during spoilage. *Food Control*, 123, Article 107697. <https://doi.org/10.1016/j.foodcont.2020.107697>
- Ma, X., Qiao, C., Wang, X., Yao, J., & Xu, J. (2019). Structural characterization and properties of polyols plasticized chitosan films. *International Journal of Biological Macromolecules*, 135, 240–245. <https://doi.org/10.1016/j.ijbiomac.2019.05.158>
- Mohajer, S., Taha, R. M., Ramli, R. B., & Mohajer, M. (2016). Phytochemical constituents and radical scavenging properties of *Borago officinalis* and *Malva sylvestris*. *Industrial Crops and Products*, 94, 673–681. <https://doi.org/10.1016/j.indcrop.2016.09.045>
- Nguyen, T. T., Pham, B.-T. T., Nhin Le, H., Bach, L. G., & Thuc, C. N. H. (2022). Comparative characterization and release study of edible films of chitosan and natural extracts. *Food Packaging and Shelf Life*, 32, Article 100830. <https://doi.org/10.1016/j.fpsl.2022.100830>
- Peinado, I., Koutsidis, G., & Ames, J. (2016). Production of seafood flavour formulations from enzymatic hydrolysates of fish by-products. *LWT- Food Science and Technology*, 66, 444–452.
- Qiu, D., Duan, R., Wang, Y., He, Y., Li, C., Shen, X., & Li, Y. (2023). Effects of different drying temperatures on the profile and sources of flavor in semi-dried golden pompano (*Trachinotus ovatus*). *Food Chemistry*, 401, Article 134112. <https://doi.org/10.1016/j.foodchem.2022.134112>
- Shemshad, S., Kamali, S., Khavandi, A., & Azari, S. (2018). Synthesis, characterization and in-vitro behavior of natural chitosan-hydroxyapatite-diopside nanocomposite scaffold for bone tissue engineering. *International Journal of Polymeric Materials and*

- Polymeric Biomaterials*, 68(9), 516–526. <https://doi.org/10.1080/00914037.2018.1466138>
- Siripatrawan, U., & Vitchayakitti, W. (2016). Improving functional properties of chitosan films as active food packaging by incorporating with propolis. *Food Hydrocolloids*, 61, 695–702. <https://doi.org/10.1016/j.foodhyd.2016.06.001>
- Sun, L., Sun, J., Chen, L., Niu, P., Yang, X., & Guo, Y. (2017). Preparation and characterization of chitosan film incorporated with thinned young apple polyphenols as an active packaging material. *Carbohydrate Polymers*, 163, 81–91. <https://doi.org/10.1016/j.carbpol.2017.01.016>
- Verma, R., Mishra, S. R., Gadore, V., & Ahmaruzzaman, M. (2023). Hydroxyapatite-based composites: Excellent materials for environmental remediation and biomedical applications. *Advances in Colloid and Interface Science*, 315, Article 102890. <https://doi.org/10.1016/j.cis.2023.102890>
- Vijayakumar, R., Sivaraman, Y., Pavagada Siddappa, K. M., & Dandu, J. P. R. (2022). Synthesis of lignin nanoparticles employing acid precipitation method and its application to enhance the mechanical, UV-barrier and antioxidant properties of chitosan films. *International Journal of Polymer Analysis and Characterization*, 27(2), 99–110. <https://doi.org/10.1080/1023666X.2021.2016305>
- Wang, W., Liu, Y., Liu, A., Xiao, J., Wang, K., Zhao, Y., & Zhang, L. (2016). Fabrication of acid-swollen collagen Fiber-based composite films: Effect of Nano-hydroxyapatite on packaging related properties. *International Journal of Food Properties*, 20. <https://doi.org/10.1080/10942912.2016.1190745>
- Wei, P., Zhu, K., Cao, J., Dong, Y., Li, M., Shen, X., & Li, C. (2021). The inhibition mechanism of the texture deterioration of tilapia fillets during partial freezing after treatment with polyphenols. *Food Chemistry*, 335, Article 127647. <https://doi.org/10.1016/j.foodchem.2020.127647>
- Wu, C., Li, Y., Wang, L., Hu, Y., Chen, J., Liu, D., & Ye, X. (2016). Efficacy of chitosan-Gallic acid coating on shelf life extension of refrigerated Pacific mackerel fillets. *Food and Bioprocess Technology*, 9(4), 675–685. <https://doi.org/10.1007/s11947-015-1659-9>
- Xie, Q., Liu, G., & Zhang, Y. (2022). Edible films/coatings containing bioactive ingredients with micro/nano encapsulation: A comprehensive review of their fabrications, formulas, multifunctionality and applications in food packaging. *Critical Reviews in Food Science and Nutrition*, 1–38. <https://doi.org/10.1080/10408398.2022.2153794>
- Xiong, Y., Kamboj, M., Ajlouni, S., & Fang, Z. (2021). Incorporation of salmon bone gelatine with chitosan, gallic acid and clove oil as edible coating for the cold storage of fresh salmon fillet. *Food Control*, 125. <https://doi.org/10.1016/j.foodcont.2021.107994>
- Ye, J., Wang, S., Lan, W., Qin, W., & Liu, Y. (2018). Preparation and properties of polylactic acid-tea polyphenol-chitosan composite membranes. *International Journal of Biological Macromolecules*, 117, 632–639. <https://doi.org/10.1016/j.ijbiomac.2018.05.080>
- Yu, Z., Jiang, Q., Yu, D., Dong, J., Xu, Y., & Xia, W. (2022). Physical, antioxidant, and preservation properties of chitosan film doped with proanthocyanidins-loaded nanoparticles. *Food Hydrocolloids*, 130. <https://doi.org/10.1016/j.foodhyd.2022.107686>
- Zhang, L., Chen, D., Yu, D., Regensteine, J. M., Jiang, Q., Dong, J., & Xia, W. (2022). Modulating physicochemical, antimicrobial and release properties of chitosan/zein bilayer films with curcumin/nisin-loaded pectin nanoparticles. *Food Hydrocolloids*, 133. <https://doi.org/10.1016/j.foodhyd.2022.107955>
- Zhang, W., Jiang, H., Rhim, J. W., Cao, J., & Jiang, W. (2023). Tea polyphenols (TP): A promising natural additive for the manufacture of multifunctional active food packaging films. *Critical Reviews in Food Science and Nutrition*, 63(2), 288–301. <https://doi.org/10.1080/10408398.2021.1946007>
- Zhang, Z., Meng, Y., Wang, J., Qiu, C., Miao, W., Lin, Q., & Jin, Z. (2024). Preparation and characterization of zein-based core-shell nanoparticles for encapsulation and delivery of hydrophobic nutrient molecules: Enhancing environmental stress resistance and antioxidant activity. *Food Hydrocolloids*, 148, Article 109524. <https://doi.org/10.1016/j.foodhyd.2023.109524>
- Zhou, X., Liu, X., Wang, Q., Lin, G., Yang, H., Yu, D., & Xia, W. (2022). Antimicrobial and antioxidant films formed by bacterial cellulose, chitosan and tea polyphenol – Shelf life extension of grass carp. *Food Packaging and Shelf Life*, 33, Article 100866. <https://doi.org/10.1016/j.fpsl.2022.100866>